Optical Beat Noise Suppression and Power Equalization in Subcarrier Multiple Access Passive Optical Networks by Downstream Feedback

S. Soerensen

***Abstract*—This paper describes a cost-effective method of suppressing optical beat noise in subcarrier multiple access passive optical networks. The method is based on initial power equalization followed by automatic fine tuning of laser wavelengths, via downstream feedback control of their mean powers, so that the receiver noise floor level is continously minimized. Application and performance of the method is demonstrated for a low-cost 16-channel system with uncooled Fabry–Perot lasers, utilizing narrow-band QPSK modulated subcarrier frequencies over more than one octave. In static and dynamic temperature worst-case situations a considerable reduction in the number of transmission errors caused by optical beat noise is observed, depending on the temperature change rate.**

***Index Terms*—Downstream feedback, optical beat interference (OBI), optical beat noise (OBN), passive optical network (PON), power equalization, quarternary phase shift keying (QPSK), subcarrier multiple access (SCMA).**

I. Introduction

OPTICAL beat interference (OBI) arises due to the quadratic conversion of optical to electrical power by mixing of optical fields when two or more light sources illuminates a receiver photodiode at the same time. OBI may be controlled and utilized for communication in systems with coherent detection, but in a subcarrier multiple access (SCMA) passive optical network (PON) it may cause unwanted disturbing products in the electrical frequency range used for the subcarriers. It is then denoted optical beat noise (OBN). A mathematical description is beyond the scope of this paper but may be found in [1], [2] and [3]. The parameters affecting the amount of OBN in a SCMA-PON are summarized as follows:

- number, type, and power of the optical sources;
- spectral distribution of the optical sources;
- wavelength separation of the optical spectra;
- number and linewidth of longitudinal modes for lasers;
- polarization of the individual optical modes;
- data bit rate and modulation format;
- subcarrier frequency and modulation index.

According to [1] the signal-to-interference ratio (SIR) is proportional to the square of the modulation index $(m \leq 1)$ and inversely proportional to the receiver bandwidth (B). Having chosen the number and type of optical sources and the receiver bandwidth for a given data bitrate and modulation format, the remaining methods of minimizing OBN may be divided into two main categories.

1) *Spectral Broadening:*
   - Light-emitting diodes (LEDs) as optical sources. The low output power limits the split ratio and transmission distance in the PON.
   - Direct intensity laser modulation index $m > 1$. Limits the usable subcarrier frequency range due to harmonics.
   - Very high subcarrier modulation frequencies. Increases the cost of the transmitter and receiver.
   - Very high frequency laser chopping. Increases the cost of the transmitter and receiver.
2) *Wavelength Separation:*
   - Laser selection by wavelength. Expensive, requires laser temperature control for multichannel field systems.
   - Laser temperature control. Expensive, requires a record of wavelengths/temperatures for replacement or addition.
   - Automatic wavelength control. Requires feedback from the receiver to each of the transmitters.

II. Downstream Feedback

The method described here belongs to the second category. It is aimed particulary at low cost bidirectional PONs with upstream SCMA, requiring low subcarrier harmonic levels over a large optical dynamic range $(m < 1)$, using direct current/intensity modulated standard multimode Fabry–Perot lasers without temperature control or special wavelength selection. However, it may also be used in systems where the modulation index is larger than 1 and in systems with temperature stabilization of the lasers.

According to [4] the dynamic range of a SCMA-PON using Fabry–Perot lasers becomes very small in the presence of OBN when the laser modulation index is less than 1. Furthermore the attenuation may be different for each branch in a practical PON. The method therefore includes initial power equalization of the received subcarrier levels at system start-up. This is followed by automatic fine tuning of the laser wavelengths, via downstream feedback control of their optical mean powers, performed on the basis of noise measurements in a frequency band not used for subcarriers. This procedure minimizes the receiver noise floor level continously during operation. It will improve the SIR and

Manuscript received December 20, 1999; revised June 2, 2000. This work is a part of the ACTS-038 project, which was supported by the EU.

The author is with the R&D Tellabs Denmark A/S, Ballerup 2750 Denmark.

Publisher Item Identifier S 0733-8724(00)09106-4.

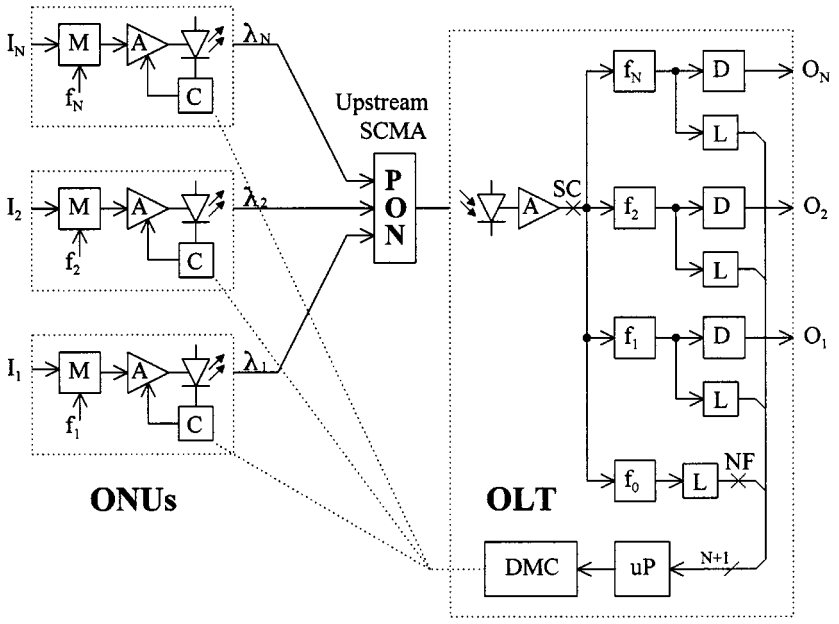

Fig. 1. Principle of downstream feedback.

reduce the number of transmission errors caused by OBN in systems where the following assumptions hold true.

The small relative changes in the optical mean powers will increase the distance between interfering modes sufficiently without substantially changing the subcarrier power level. Additionally, the laser linewidths are large enough to cause a noise reduction in the subcarrier frequency band as well as the measurement frequency band.

In Fig. 1 a PON provides upstream SCMA for a number (N) of remote optical network units (ONUs), with standard lasers transmitting on the wavelengths $\lambda_1, \lambda_2, \ldots \lambda_N$. In each ONU the optical output mean power is controlled via the laser bias current by the circuit C, which also controls the laser modulation current via the variable amplifer A. The subcarrier frequencies $f_1, f_2, \ldots f_N$ are modulated with the input signals $I_1, I_2, \ldots I_N$ in the modulators (M).

In the optical line terminal (OLT) of the head-end the photodiode converts the sum of optical signals to an electrical signal, which is amplified in A and separated by a set of filters or heterodyne receivers on the subcarrier frequencies $f_1, f_2, \ldots f_N$. The output signals $O_1, O_2, \ldots O_N$ are recovered from the subcarriers by the demodulators (D).

Subcarrier power equalization at the point SC is done at system start-up by means of level detectors (L) on the filter outputs, providing feedback to the power and modulation controls of the ONUs, via the microprocessor (μP) and the downstream management channels (DMCs). Subsequently, the receiver noise floor level is continuously measured in some free bandwidth not used for subcarriers and separated from these by a filter f_0. The filtered noise is applied to another level detector (L), the output of which (the point NF) is used to control the laser mean powers of the ONUs. This is also done via the μP and the DMC, in accordance with the OBN suppression algorithm described below.

III. OBN Suppression

The basic idea of wavelength control by feedback based on out-of-band noise measurements is described in [5] but it does not account for power equalization or harmonics control which are essential issues in real multi-octave SCMA systems with large differencies in their optical branch attenuations. Furthermore, the algorithm proposed in [5], which is based on temperature control, would be very slow, power consuming and expensive to implement, and it has never been verified.

Fig. 1 is an enhancement of the principle described in [5] incorporating arrangements for subcarrier power equalization controlling harmonics by calibration of the ONUs. In addition the new OBN algorithm described below and illustrated by the flow-chart in Fig. 2 solves the earlier problems.

Initially, equalization is done for each of the calibrated ONUs in turn by gradually increasing the optical mean power $P_0(n)$ and modulation $P_1(n)$ until the nominal level L_N is reached on the subcarrier level detector. The upstream management channel is then verified to be operational before the corresponding nominal mean power $P_N(n)$ is stored and the status $\mathrm{ST}(n)$ set to active. A number of active ONUs, capable of transmitting management information and acknowledging commands from the OLT, are then available.

The subsequent OBN suppression process is essentially a continously repeated moving window minimum search within specified limits of optical mean power for each of the active ONUs in turn. The limits (P_{L+} to P_{L-}) are calculated as a factor K_L relative to $P_N(n)$. In each cycle $P_0(n)$ is stepped with P_S through a power window and set to the value P_M causing the minimum output NF_M at the receiver noise level detector. The window size (P_{W+} to P_{W-}) is calculated as a factor $K_W < K_L$ relative to the minimum found in the previous cycle for that ONU, starting with $P_N(n)$ immediately after equalization.

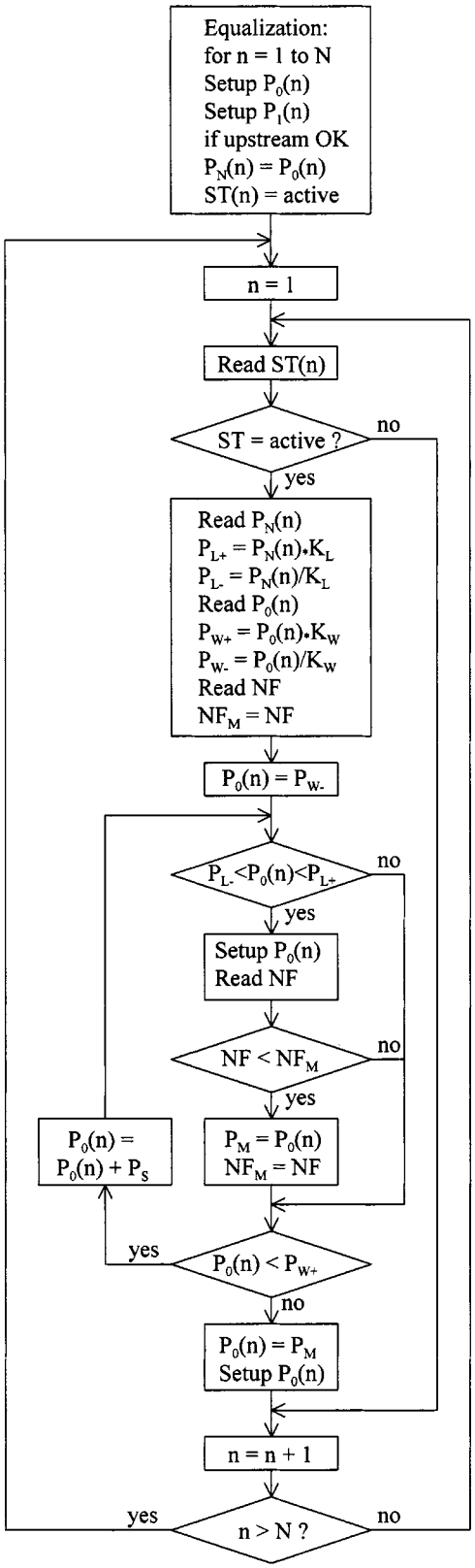

Fig. 2. OBN suppression algorithm.

This procedure allows the mean powers, and thereby the wavelengths, of the active ONUs to move around within the specified limits in a continuous search for the combination providing the lowest receiver noise floor level at f_0.

In the absence of OBN the nominal mean power settings should remain unchanged. When OBN appears it should be suppressed by the algorithm with an effeciency depending on the rate of change in the OBN level and the time it takes to perform a window sweep for all ONUs in the PON.

Besides the excecution speed, the efficiency of the OBN suppression algorithm also depends on the size of the sweep window and the limits of the allowed mean power deviation. If K_W is small, the probability of being caught in a local minimum is larger, but if K_W approaches K_L a mean power value causing a higher level of OBN is more likely to be tested during the sweep of an ONU.

IV. Power Equalization

When modulated with a sinusodial subcarrier of frequency f_C the laser output power of the ONU is given by

$$P(t) = P_0 + P_1\cos(2\pi f_C t) + P_2\cos(4\pi f_C t) + \cdots \quad (1)$$

The optical modulation index m and relative second-harmonic level s is given by

$$m = \frac{P_1}{P_0} \quad (2)$$

and

$$s = \frac{P_2}{P_1}. \quad (3)$$

For an ideal laser diode the higher order terms in (1) are zero in the linear region above threshold. For real laser diodes the nonlinearity is most significant just above threshold, which means that for a fixed modulation index the harmonic distortion will increase with decreasing mean output power.

In SCMA systems operating over more than one octave harmonics must be limited to a nondisturbing level and thus only values of $m < 1$ are allowed. However, in order to spread the spectra and minimize initial OBN, m should be as large as possible over the dynamic range, without causing excessive harmonics even if the mean power is reduced by the factor K_L in the subsequent OBN suppression process. Empirically a suitable compromise is obtained by setting the optical mean power P_0 versus optical path attenuation A according to

$$P_0(A) = a \cdot A + b \quad (4)$$

Inserting the limits of the dynamic range $P_{0,\min} = P_0(A_{\min})$ and $P_{0,\max} = P_0(A_{\max})$ and solving for a and b yields

$$P_0(A) = P_{0,\max} - \frac{P_{0,\max} - P_{0,\min}}{A_{\max} - A_{\min}}(A_{\max} - A) \quad (5)$$

If $P_0(A)/K_L = P_{02}(A)$ is the optical mean power causing a second harmonic level of $10\log(s) = 10\log(P_2/P_1) = -S$ dBc after power equalization, then (5) may be written:

$$P_0(A) = K_L\left[P_{02,\max} - \frac{P_{02,\max} - P_{02,\min}}{A_{\max} - A_{\min}}(A_{\max} - A)\right] \quad (6)$$

and the calibration procedure below may be used to determine the values of $P_{02,\min}$ and $P_{02,\max}$ individually for each laser as follows:

- for $A_{\min}$ setup the maximum allowed laser mean power;
- increase the modulation current I_1 until the nominal subcarrier level L_N is reached in the receiver;
- reduce the mean power to the level $P_{02,\min}$ for which the second harmonic is $2*S$ dB below the carrier measured at the SC point in Fig. 1, while readjusting the modulation to maintain L_N if necessary, and note the final setting $I_{1,\min}$;
- repeat the above procedure for $A_{\max}, P_{02,\max}$ and $I_{1,\max}$.

The required modulation current versus optical attenuation is

$$I_1(A) = \frac{I_{1,\max}}{A_{\max}} \cdot A \tag{7}$$

and the gradual increase of mean power and modulation during power equalization may then be done according to (6) and (7) starting with $A = A_{\min}$ and increasing A stepwise until the nominal receiver subcarrier level L_N is reached.

If the laser temperature is held constant, or the modulation current amplitude is properly compensated for the change in the P/I slope with temperature, the calibration procedure will ensure optical second harmonic levels less than $-S$ dBc within the dynamic range during the subsequent execution of the OBN suppression algorithm.

Now, if the downstream traffic is carried in the same fibers as the upstream traffic, by means of bidirectional optical devices in the OLT and the ONUs, then the optical attenuation is the same in both directions and it may be calculated as

$$A = \frac{P_T}{P_R} \tag{8}$$

where P_T is the constant optical mean power transmitted by the OLT and P_R is the received optical mean power in the ONU. Substituting (8) into (6) yields

$$P_0(P_R) = K_L \left[P_{02,\max} - \frac{P_{02,\max} - P_{02,\min}}{\frac{1}{P_{R,\min}} - \frac{1}{P_{R,\max}}} \left(\frac{1}{P_{R,\min}} - \frac{1}{P_R} \right) \right]. \tag{9}$$

An alternative way of performing power equalization is therefore first to measure P_R, then setting $P_0(P_R)$ according to (9) and finally increasing the modulation current I_1 stepwise until the the nominal receiver subcarrier level L_N is reached.

However, this could cause more optical interference with other channels when a new ONU is added to a system during operation, since the optical mean power is applied before the modulation is turned on. From this point of view it is probably better to slowly increase the mean power and modulation simultaneously according to (6) and (7), allowing the OBN suppression process more time to work on the active ONUs.

V. System Design

This section describes how the principles of power equalization and OBN suppression by downstream feedback are implemented in a 16 channel narrow-band SCMA-PON with downstream Time Division Multiplexing (TDM).

The PON carries the downstream traffic at 1550 nm in the same fibers as the upstream traffic at 1300 nm by means of bidirectional optical devices (BIDIs) in the OLT and ONUs. This minimizes the interference from optical reflections.

The BIDIs include a receiver p-i-n-diode, a Fabry–Perot laser diode, an output power monitor diode, a wavelength division multiplexer (WDM) to separate 1300 from 1550 nm, and a single-mode fiber for the common input and output. There is no internal peltier-element or temperature sensor, so the laser temperature is allowed to drift. However, an external sensor measures the temperature of the housing.

The mean output power P_0 is set by comparing the monitor diode current with a programmable reference. Therefore it is practically temperature independent, whilst the laser bias current I_0 increases with temperature. The sinusodial modulation current amplitude I_1 in the ONU and the peak pulse current in the OLT is compensated for the change in the laser P/I slope with temperature, by means of the external sensor. This is done in order to achieve a practically temperature independent modulation index in the ONU and extinction ratio in the OLT.

The 1550-nm laser in the OLT is nonreturn-to-zero (NRZ) modulated with 155.52 Mb/s downstream data. In each of the 16 ONUs the 1300 nm laser is modulated with a subcarrier in the frequency range 80–230 Mhz. The subcarrier is QPSK modulated with the 4.86 Mb/s narrowband I/Q symbol rate from the coded demultiplexed 9.72 Mb/s upstream data.

Management data at 768 kb/s is embedded in the 155.52 Mb/s TDM downstream data, from which a clock is recovered and used for upstream timing in each ONU. Similary, a 64 kb/s management channel is embedded in the 9.72 Mb/s upstream data of each ONU prior to QPSK modulation.

Selectivity of the subcarrier filters in the OLT is obtained in heterodyne receivers where the subcarrier f_C, by means of a programmable local oscillator at f_L, is down converted to an intermediate frequency f_I which is then QPSK demodulated.

Level detection is done at the intermediate frequency and clock recovery acquisition, phase alignment, I/Q ambiguity resolution and multiplexing into 9.72 Mb/s is done in a custom device for all 16 channels. Further description of the digital signal processing in the OLT and ONU, is beyond the scope of this paper.

A. Frequency Plan

QPSK modulation was chosen as a suitable compromise between the transmission channel bandwidth, the subcarrier phase noise requirements and the availability and cost of components for digital radio equipment on the market.

The subcarrier frequencies may be written: $f_C = f_X + n \cdot f_S$, for $n = 1$ to 16, where f_X is the offset and f_S is the channel spacing. To allow for uncritical transmitter I/Q filtering f_S was set to 9.72 MHz. The offset was chosen so that second harmonics of lower carriers are placed exactly between higher carriers and third harmonic of the lowest carrier is above the highest carrier, which implies that $f_X = 7.5 \cdot f_S = 72.9$ MHz.

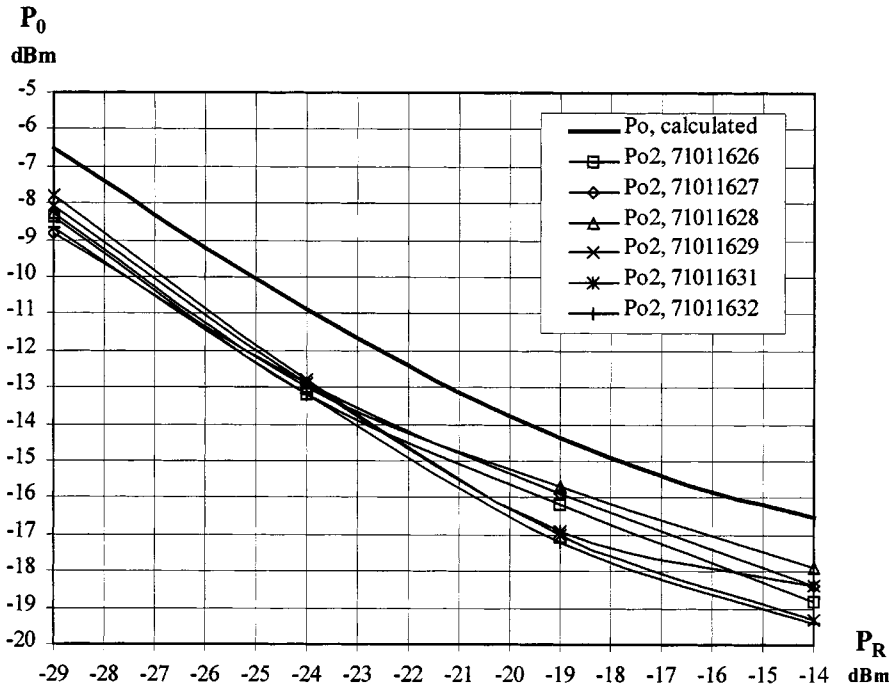

Fig. 3. ONU output power versus input power.

TABLE I

Channel No.	Carrier f_C	Local f_L	Image $f_L + f_I$	2. Harm $2 \cdot f_C$	1. Spur $2 \cdot f_L - f_I$
1	82.62	152.62	222.62	165.24	235.24
2	92.34	162.34	232.34	184.68	254.68
3	102.06	172.06	242.06	204.12	274.12
4	111.78	181.78	251.78	223.56	293.56
5	121.50	191.50	261.50	243.00	313.00
6	131.22	201.22	271.22	262.44	332.44
7	140.94	210.94	280.94	281.88	351.88
8	150.66	220.66	290.66	301.32	371.32
9	160.38	230.38	300.38	320.76	390.76
10	170.10	240.10	310.10	340.20	410.20
11	179.82	249.82	319.82	359.64	429.64
12	189.54	259.54	329.54	379.08	449.08
13	199.26	269.26	339.26	398.52	468.52
14	208.98	278.98	348.98	417.96	487.96
15	218.70	288.70	358.70	437.40	507.40
16	228.42	298.42	368.42	456.84	526.82

Finally $f_I = 70$ MHz was chosen, for which compact SAW filters are available, and f_L was placed above f_C in order to separate spurious. This determines the (MHz) frequency plan.

Since the heterodyne receivers are just as sensitive to the image as to the carrier, the range is split with filters after the SC point into a low band (1–8) and a high band (9–16).

Noise floor measurements are done below the subcarrier range, where the receiver thermal noise is smallest, at $f_0 = 70$ MHz through a SAW filter similar to the ones used at f_I. A logarithmic detector with a 17-mV/dB response is used, so an increase of 100 mV at the NF point indicates a rise of approximate 6 dB in the receiver noise floor at 70 MHz at the SC point.

B. Dynamic Range

As a design target the SCMA-PON should work error-free in the absence of OBN with attenuations of 10 to 25 dB in the optical paths between the OLT and the ONUs. Equalization according to (9) is used and since the constant OLT output mean power is $P_T = -4.0$ dBm the received ONU mean power P_R will be between -14 and -29 dBm.

In order to determine the ONU mean output power P_{02} required to keep the optical second harmonics below -10 dBc (-20 dBc at the SC point) the calibration procedure is applied to 6 different ONUs at four points within the dynamic range. The results are plotted in Fig. 3 for each of their serial numbers.

Though it is possible to store individual values for the dynamic range limits in each ONU, the worst case values: $P_{02,\max} = -7.8$ dBm and $P_{02,\min} = -17.8$ dBm are used generally. With $K_L = 1.35$, corresponding to an allowed mean power deviation of $\pm 10 \cdot \log K_L = \pm 1.3$ dB, $10 \cdot \log P_0(P_R)$ is calculated according to (9) in units of dBm and plotted in Fig. 3.

The distance of 1.3 dB between P_0 and P_{02} in the end points is fairly constant for points within the dynamic range as well, which justifies the assumption in (4) and the use of (9).

C. OBN Algorithm Monitor

From the OLT it is possible to monitor all settings and measured values in the system during operation. The OBN algorithm monitor shows information from all ONUs on their types, status, Bit Interleaved Parity (BIP) error counts, received powers, nominal output powers and actual output power deviations. It also includes readout of the actual subcarrier and noisefloor levels in the OLT. Further, it is possible to set the parameters K_L and

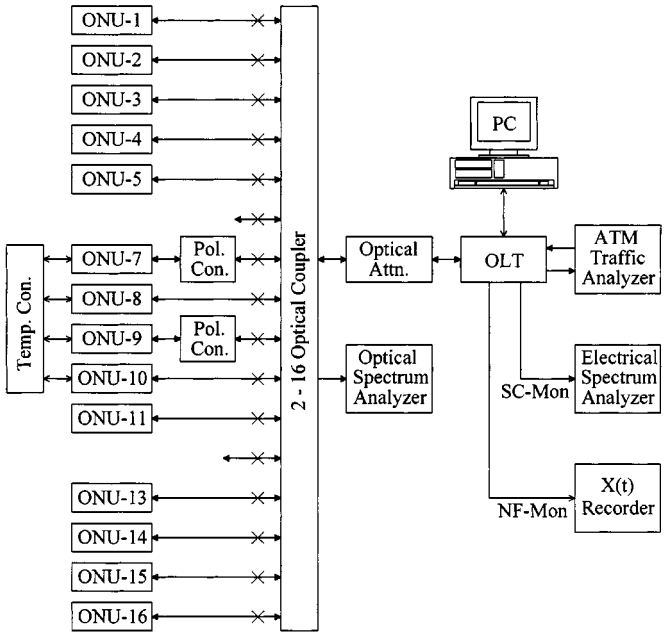

Fig. 4. OBN test setup for APON system.

K_W, to start/stop the algorithm and to reset output powers to their nominal values.

VI. OBN System Tests

The SCMA front-ends described above are used in two different types of access systems: the synchronous-PON (SPON), where each 9.72 Mb/s channel transports 4 multiplexed 2.352 Mb/s SDH VC12s, and the asynchronous-PON (APON), where each 9.72 Mb/s channel transports 9.3 Mb/s ATM traffic. The APON system is used for verification.

Fig. 4 shows the OBN test setup for the APON system. Only 14 ONUs were available at the time of testing. These are connected to the OLT and to an optical spectrum analyzer via a 2–16 coupler with an optical attenuation of appx. 12–13 dB. A variable optical attenuator is inserted between the coupler and the OLT, and fixed optical attenuators may be inserted between the coupler and the ONUs as marked with an X.

An electrical spectrum analyzer is connected to the OLTs subcarrier monitor point, and an $X(t)$ recorder is connected to its noise floor monitor point. A Personal Computer with a terminal program is used to control and monitor the system.

An ATM traffic analyzer for measuring PRBS errors in the payload of the 9.3 Mb/s traffic is connected to the OLT and traffic loop-back is applied in the ONU to be measured. In this application, the payload of the ATM-cell is 47 bytes out of 53, so a PRBS error count of 1/min corresponds to an error rate of $(60 \cdot 9.3 \cdot 10^6 \cdot 47/53)^{-1} = 2.0209 \cdot 10^{-9}$.

Optical beat noise is generated by temperture control of the laser wavelengths in 4 selected ONUs, and polarization controls are used to maximize the OBN for worst-case measurements. The temperature controls consist of external peltier-elements with heatsinks and temperature sensors clamped to the laser housings of the ONUs. These are connected to a 4-channel control box where the temperatures can be set individually between

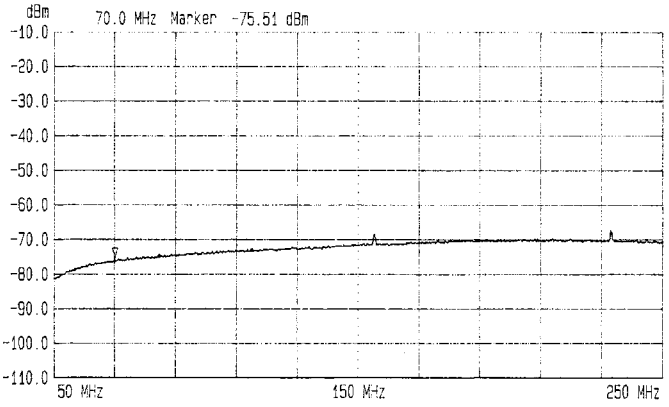

Fig. 5. Receiver noise floor.

25 and 75°C. The control box includes an offset voltage generator with dV/dt limitation, so that a sweep around the preset temperature value, with a selectable rate of 2, 5, 10, 20, 50 or 100 °C/h, may be performed for one or more of the ONUs at the same time.

A. Noise Floor and Harmonics

In these and all of the following measurements with the electrical spectrum analyzer, the resolution bandwidth is 500 kHz, the video bandwidth is 1 kHz and the sweep time 1.22 s for a sweep from 50 to 250 MHz.

Fig. 5 shows the receiver noise floor measured without optical input to the OLT. In the subcarrier range from 80 to 230 MHz the noise floor increases from −75 dBm to −70 dBm. This is a property of the p-i-n diode, while the rolloff below 70 MHz and above 240 MHz is due to filtering after the transimpedance amplifier. At 70 MHz, the receiver noise floor is −75.5 dBm corresponding to a reading of 700 mV in the NF monitor point.

Fig. 6 shows subcarriers 1–5 and their second harmonics after equalization with appx. 24–25 dB of optical attenuation and the OBN algorithm disabled. The channel peak level is appx. −45 dBm corresponding to a reading of appx. 22 mV on the subcarrier level detectors. Even though these are not the same ONUs as used for the measurements in the previous section, the second harmonics are still more than 20 dB below the subcarriers.

B. OBN Generation and Suppression

Due to differencies in mode spacing and mode jumping, which occurs during temperature changes, it is a difficult and time consuming task to find more than two ONU lasers with coincident main modes in the 25 to 75 °C temperature range. Therefore, the 4 ONUs used to generate optical beat noise are selected to form two pairs 7–8 and 9–10 with coincident main modes at some preset temperatures. Initially this is done after equalization with the optical attenuator set to 5 dB.

Figs. 7 to 11 show the optical spectra of channels 7, 8, 9, and 10 both separately and together at the preset temperatures of main mode coincidence. The pair 7–8 has coincident main modes at 1319.26 nm and the pair 9–10 at 1329.20 nm. Fig. 12 shows the optical spectra of all 14 channels simultaneously as they appear in the subsequent static temperature tests.

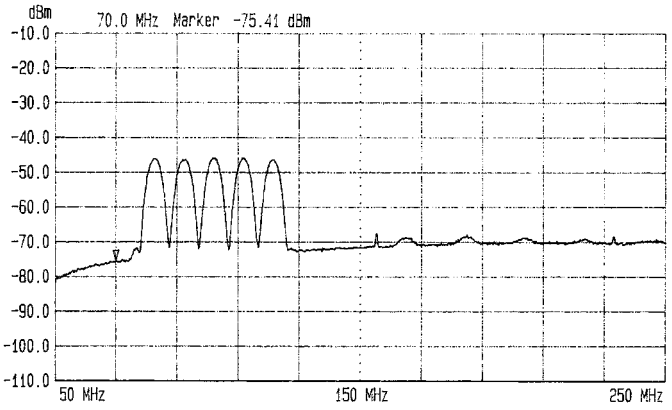

Fig. 6. Harmonics of Channels 1–5.

Fig. 13 shows subcarriers 7–10 after equalization with approximately 18–19 dB of optical path attenuation and adjustment of the polarization controls for maximum OBN. The noise floor level is −58 dBm at 70 MHz. Fig. 14 shows subcarriers 7–10 after the OBN algorithm has been activated and allowed to settle with $K_L = 1.4$ and $K_W = 1.1$. The noise floor is level was reduced 16.5 dB at 70 MHz and 10.5 dB at 230 MHz down to approximately 1 dB above the level in Fig. 5. There were no significant changes in the received subcarrier levels and during the settling process the BIP errors were reduced to zero in all four channels. This confirms the basic principles and assumptions.

Results from the OBN algorithm monitor are shown in Table II. P_R is the received power, $P_0(P_R)$ is the nominal power after equalization according to (9) and ΔP_0 is the power change from Figs. 13 to 14. The noise minimum was found within the allowed limits for the beating pair of lasers 7–8 while the beating pair of lasers 9–10 were driven to their limits $10 \log K_L = \pm 1.5$ dB. However, increasing K_L did not improve the noise reduction significantly and emperically values of around 1.3 to 1.4 was found to give satisfactory results.

VII. Static Temperature Tests

The purpose of the tests in this section is to examine how a system with 14 ONUs handles a static temperature "worst-case" situation when the OBN algorithm is activated after power equalization with values of optical path attenuations in the specified dynamic range. The "worst-case" situation is generated by adjusting the temperature and polarization of the two beating pairs 7–8 and 9–10 to maximum OBN after equalization. However, the uncontrolled laser temperature of the remaining ONUs may eventually cause beating with the main or side modes of other channels, causing additional contributions to the noise floor.

A. 1 dB Attenuation Spread

Fig. 15 shows all subcarriers with "worst-case" OBN after equalization with appx. 18–19 dB of optical path attenuation. The BIP error count for the 14 active channels was between 13052 and 38 701 over one minute, during which the slightly fluctuating noise floor reached a maximum level of −57.9 dBm at 70 MHz. Fig. 16 shows all subcarriers after the OBN algorithm has been activated and allowed to settle with $K_L = 1.4$ and $K_W = 1.1$. Over one minute there were no BIP errors in any channels and the noise floor reached a maximum level of −73.3 dBm at 70 MHz, which is just 2.2 dB above the level in Fig. 5. The noise reduction was achieved without excessive second harmonics or significant changes in the received subcarrier levels. Table III shows the ONU mean output power changes from Figs. 15 to 16.

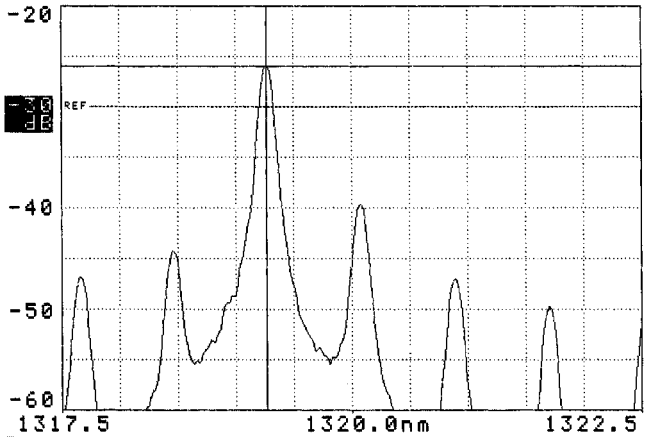

Fig. 7. Channel 7 at 35.9 °C.

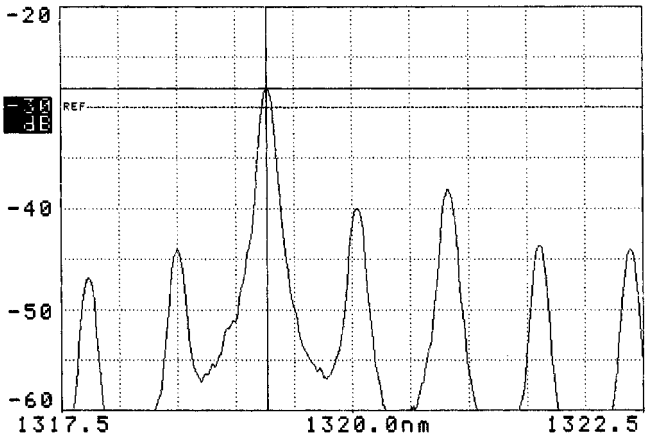

Fig. 8. Channel 8 at 50.0 °C.

B. 10 dB Attenuation Spread

To create attenuation spread fixed attenuators were inserted in some of the X points in Fig. 4. Unfortunately equalization was impossible for attenuations below 15 dB, due to insufficient resolution in the digital-to-analogue converter (DAC) setting the modulation current amplitude in the ONUs. Therefore the measurements above were repeated with 15–25 dB of optical path attenuations, with the smallest values for the controlled beating pairs 7–8 and 9–10, generating most of the OBN.

The results were very similar, except for a slightly higher noise level of −71.4 dBm at 70 MHz and a few BIP errors in five of the 14 channels after settling of the OBN algorithm. This is probably due to the fact that the absolute allowed mean power deviation is now smaller for channels 7–8 and 9–10 because of their lower nominal mean powers after equalization.

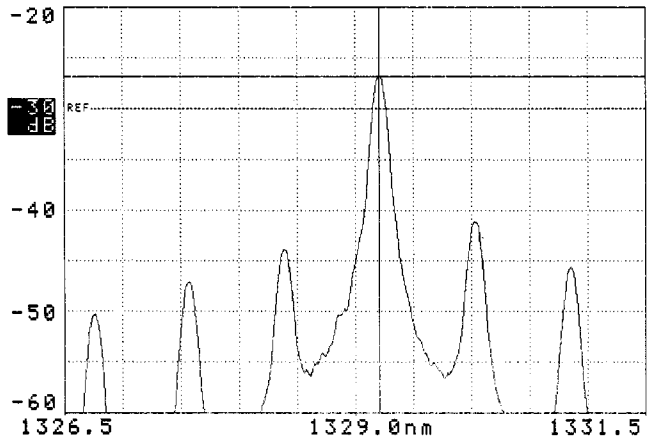

Fig. 9. Channel 9 at 65.9 °C.

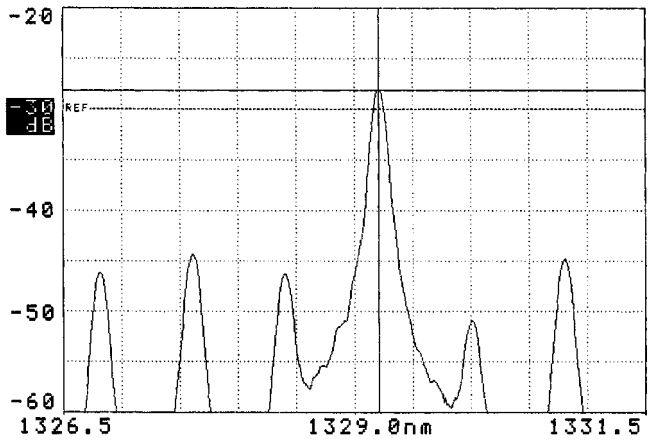

Fig. 10. Channel 10 at 50.9 °C.

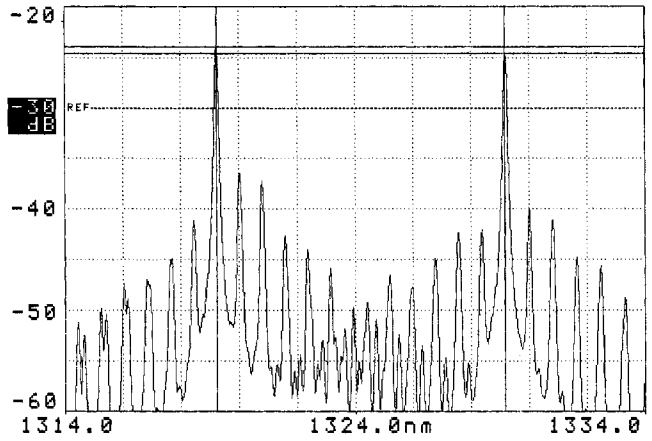

Fig. 11. Channels 7, 8, 9, and 10.

In order to extend the dynamic range over which the OBN algorithm preserves its high error reduction efficiency, this obstacle could probably be removed by using a higher value of $P_{02\,\min}$ in (9), than the one found during calibration.

C. Long-Term PRBS Error Test

This test is done to examine the error reduction speed and long-term effect of the OBN algorithm, with respect to the PRBS errors in the payload of one ATM channel, in a static "worst-case" OBN situation after equalization with 18–19 dB of optical path attenuation.

The integration period of the ATM traffic analyzer is set to 1 min and loopback of ATM cells are done in ONU-13. The "worst-case" OBN situation is created as previously stated and the error counter is started. After 10 min, the OBN algorithm is activated, allowed to settle and run for 20 min after which the monitor screen is printed out, the algorithm stopped, and the ONU mean powers reset to their nominal values. The error counter is allowed to run for another 10 min.

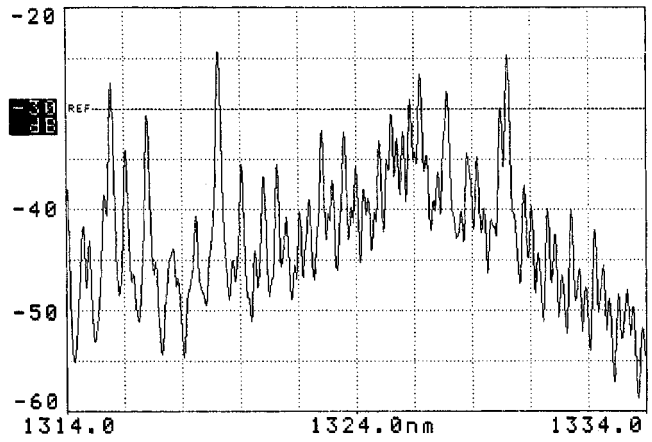

Fig. 12. All channels in test setup.

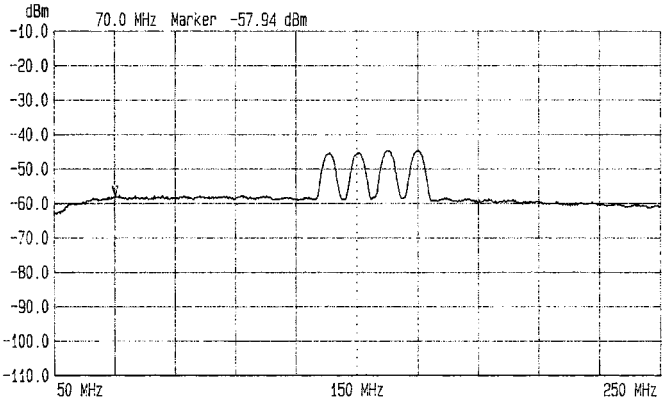

Fig. 13. Maximum OBN for two pairs beating.

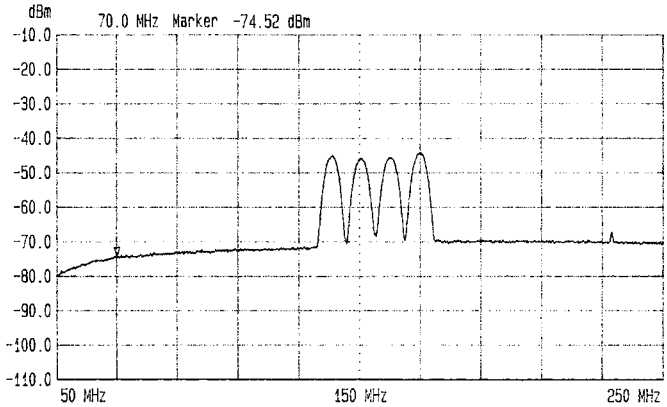

Fig. 14. OBN after settling of algorithm.

TABLE II

ONU	P_R	$P_0(P_R)$	ΔP_0
7	−22.0 dBm	−12.4 dBm	+1.4 dB
8	−22.4 dBm	−12.1 dBm	−1.3 dB
9	−23.2 dBm	−11.5 dBm	−1.5 dB
10	−23.1 dBm	−11.6 dBm	+1.5 dB

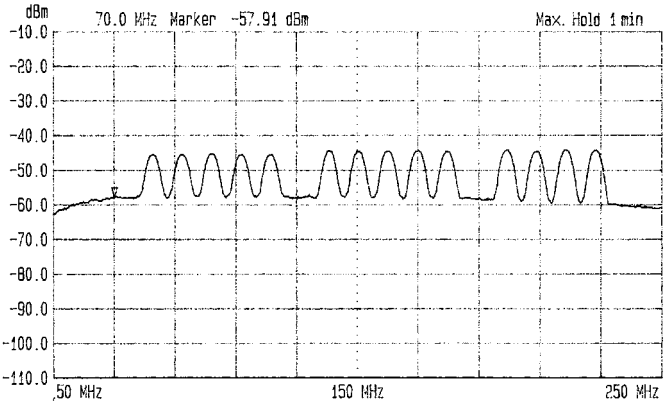

Fig. 15. "Worst-case" OBN.

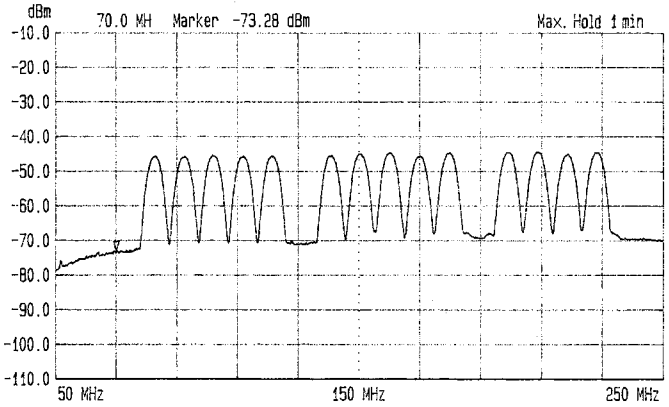

Fig. 16. OBN after settling of algorithm.

TABLE III

1:	+0.3 dB	7:	−1.2 dB	13:	−1.1 dB
2:	−0.4 dB	8:	+0.4 dB	14:	+0.8 dB
3:	−1.2 dB	9:	+1.4 dB	15:	−0.8 dB
4:	−0.7 dB	10:	−1.5 dB	16:	−0.4 dB
5:	−0.1 dB	11:	−0.9 dB		

During the first and the last 10 min periods the noise floor and error count fluctuate, but the average error ratio over these two periods together is $2.62 \cdot 10^{-3}$. In the error-free period in between, there is less than 1 error in 20 min corresponding to an error ratio of less than $1.01 \cdot 10^{-10}$. The error reduction factor of the OBN algorithm is thus at least $26 \cdot 10^{6}$times under these circumstances.

The time between window sweeps (addressing cycles) for a particular ONU is approximately 50 s and the time from activation of the OBN algorithm until the error-free noise level is reached is around 90 s. This gives an indication of the OBN algorithm execution speed, with $K_L = 1.4, K_W = 1.1$ and 14 ONUs, in this implementation.

The monitor printout after 20 min of error-free operation shows that the mean powers of all channels have been adjusted down, except channels 7 and 9 of the controlled beating pairs responsible for most of the OBN. This long-term drift toward lower power values is understandable if you consider two lasers beating with exactly coincident modes. In such a case reducing the power of a laser will be preferred, since this results in less OBN than a power increase, even if the mode wavelength step is the same size in both directions. Additionally, those lasers not beating will tend to turn their powers down to reduce intensity noise. This could be avoided by activating the algorithm only above some noise threshold. However, this long term drift does not seem to be an obstacle.

VIII. Dynamic Temperature Tests

A static temperature situation at all of the ONUs simultaneously will hardly ever occur outside the test laboratory. The purpose of the tests in this section is therefore to examine how a system with 14 ONUs handles more realistic dynamic temperature "worst-case" situations with the OBN algorithm running continously after power equalization. They are relevant for field systems, where some ONUs are inside buildings at fairly constant temperatures and others in street cabinets exposed to ambient temperature variations.

As in the previous section, the PRBS error test is done by loopback of the ATM cells in ONU-13 with an integration period of 1 min and the 'worst-case' situations are generated by adjusting temperature and polarization of the two beating pairs 7–8 and 9–10 after equalization.

With the OBN algorithm disabled a sweep of $\pm 0.5\,^{\circ}$C around the preset temperatures of the ONU lasers 7 and 10 is started simultaneously with the $X(t)$ recorder and the error counter. The sweep is repeated with the algorithm running.

During the sweeps the preset "worst-case" situation with two pairs beating is passed, but the uncontrolled laser temperature of the remaining ONUs may eventually cause beating with the main or side modes of other channels, causing additional contributions to the noise floor level.

Fig. 17 shows the noise floor voltage and the PRBS error count for a temperature sweep at 2 °C/h with the OBN algorithm disabled and running with $K_L = 1.3$ and $K_W = 1.1$. The total number of errors is 3 365 699 and 492 523 respectively, and the error reduction factor is thus 6.83 times. Single errors, corresponding to an error rate of $2 \cdot 10^{-9}$, appear around 825 mV which equals a rise of 7.5 dB up to −68.0 dBm in the noise floor level at 70 MHz. As expected the OBN algorithm has little influence on the peak noise floor level but does reduce the duration of the high noise floor level and the total number of bit errors. Since error-free transmission is achieved after appx. 90 sec. in a static "worst-case" situation, the duration of a noisefloor above 800 mV will probably not exceed the 2–3 min shown in Fig. 17 even for slower sweeps.

Fig. 18 shows the noise floor voltage and the PRBS error count for a temperature sweep at 5 °C/hour with the OBN algorithm disabled and running with $K_L = 1.3$ and $K_W = 1.1$.

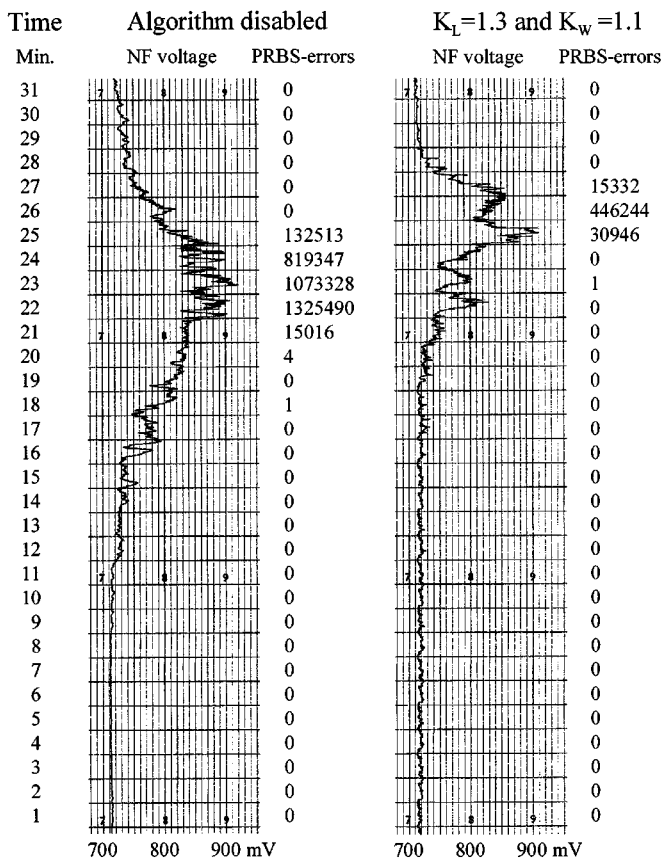

Fig. 17. Sweep at 2 °C/h.

The total number of errors is 1 158 824 and 148 539 respectively, and the error reduction factor is thus 7.80 times. This is actually better than in Fig. 17 though the duration of the high-noise floor level does not seem to be reduced much.

Fig. 19 shows the noise floor voltage and the PRBS error count for a temperature sweep at 10 °C/h with the OBN algorithm disabled and running with $K_L = 1.3$ and $K_W = 1.1$. The total number of errors is 557 873 and 344 338, respectively, and the error reduction factor is thus 1.62 times. This is not significant and the duration of the high noise floor level is practically unchanged. However, temperature changes faster than this will hardly ever occur in field applications where the enclosure thermally isolates the laser from the environment.

Repeating the measurements above reveals some spread in the calculated error reduction factors for a fixed sweep rate because it is not possible to reproduce the 'worst-case' situation exactly from sweep to sweep as the main modes of the two pairs, necessary to generate a high level of OBN, are not coincident at precisely the same time in each sweep.

It seems fair to conclude that the average error reduction factor of the OBN algorithm is 1 for temperature sweeps faster than 10 °C/h, and that it increases as the sweep speed decreases, since it is almost infinite in the static temperature situation.

It also seems resonable to assume that increasing the excecution speed of the OBN algorithm will increase the average error reduction factor and reduce the duration of the inevitable error burst during a temperature sweep at a fixed rate slower than 10 °C/h. This has not yet been verified though the system has a potential for improvements, such as follows:

- increasing OLT/ONU microprocessor calculation speed;
- increasing up- and downstream management traffic speed;
- improving the OBN algorithm, for instance by repeating the window search for an ONU, if it reduces the noise floor more than some value, before proceeding to the next.

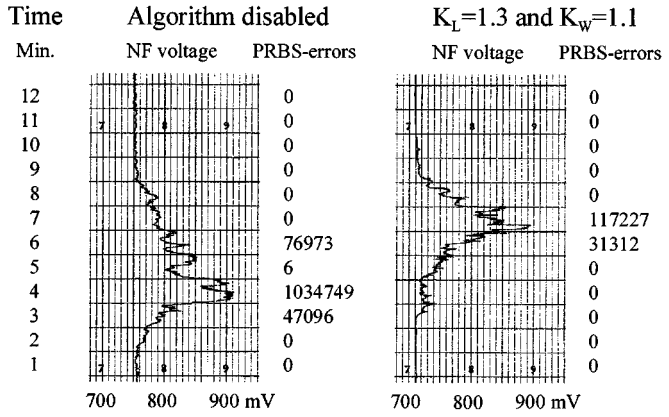

Fig. 18. Sweep at 5 °C/h.

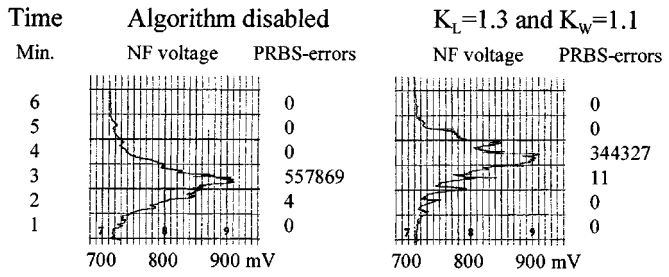

Fig. 19. Sweep at 10 °C/h.

IX. Summary

It has been shown that the principle of OBN suppression by downstream feedback may be applied successfully, taking into account subcarrier operation over more than one octave. In the APON system the OBN algorithm has an outstanding error reducing effect in static temperature "worst-case" OBN situations over an optical dynamic range of at least 10 dB, and an error ratio of less than $1 \cdot 10^{-10}$ is reached within 90 seconds from activation, for a system with 14 ONUs.

Furthermore it has been shown that the OBN algorithm in this system preserves an error reducing effect, when sweeping the temperature through "worst-case" OBN situations at rates up to 5 °C/hour. The duration of error bursts caused by slower temperature sweeps will probably always be less than 3 min and the system has a potential for improvements.

X. Conclusion

In order to achieve an optical dynamic range, which is suitable for practical purposes, power equalizing of the ONUs by downstream feedback is required anyway. Implementation of OBN suppression provides an economical extension, since it only requires an extra filter and detector in the OLT.

The "worst-case" OBN situation generated in order to test the system under static and dynamic temperature conditions is quite extreme, since it involves simultaneous wavelength and polarization coincidence of the main modes of two pairs of lasers. The probability of its occurence in field applications is therefore extremely small. However, depending on the polarization and mode distribution, there is always some risk of getting an error burst when the wavelength of one laser slowly passes the wavelength of another.

In highly demanding upstream applications this could be avoided by stabilizing all ONU lasers at the same temperature, thereby creating a static temperature situation where the OBN algorithm fine-tunes the wavelengths to obtain a minimum noise level. This increases the cost and power consumption of the system, but the benefit is that it will not be necessary to select lasers and keep a record of the wavelengths and temperatures in order to replace or add ONUs.

Tellabs APON and SPON systems utilizes retransmission in their upstream applications and they are also designed to maintain their synchronization at high bit error rates. Error bursts of some duration may therefore be tolerated and temperature control is not needed. Here the OBN suppression algorithm provides a guarantee against high bit error rates for long periods of time and results in very reliable low-cost systems for less demanding traffic.

Finally, OBN suppression by downstream feedback may also be utilized in conjunction with the spectral broadening methods for further error reductions. Therefore it constitutes a valuable contribution to the discusssion regarding the pros and cons of SCMA versus alternatives such as TDMA for the upstream traffic in bi-directional PON transport systems.

ACKNOWLEDGMENT

The author wish to thank all members of the Broadband-Loop group in Tellabs Denmark A/S for their contributions and support.

REFERENCES

[1] C. Desem, "Optical interference in subcarrier multiplexed systems with multiple optical carriers," *IEEE J. Select. Areas Commun.*, vol. 8, no. 7, pp. 1290–1295, Sept. 1990.

[2] C. Desem, "Measurement of optical interference due to multiple optical carriers in subcarrier multyiplexing," *IEEE Photon. Technol. Lett.*, vol. 3, pp. 387–389, Apr. 1991.

[3] C.-H. Chang, "Interference of multiple optical carriers in subcarrier-multiplexed systems," *IEEE Photon. Technol. Lett.*, vol. 5, pp. 848–850, July 1993.

[4] R. D. Feldman, T. H. Wood, G. Raybon, and R. F. Austin, "Effect of optical beat interference on the dynamic range of a subcarrier multiple access passive optical network using Fabry–Perot lasers," *J. Lightwave Technol.*, vol. 14, no. 5, pp. 711–715, May 1996.

[5] W. H. Powell, "Optical Network," U.K. Patent Application GB 2294372 A, Apr. 24, 1996.

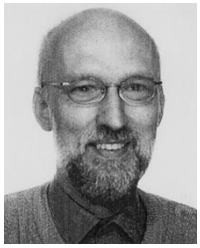

S. Soerensen was born in Copenhagen, Denmark, in 1949. He received his M.Sc. degree in electronic engineering at the Technical University of Denmark in 1980.

From 1969 to 1973, he worked as a Wireless Operator and from 1980 to 1985, he was with Skanti A/S and Storno A/S, where he worked with wireless communication systems. In 1985, he joined NKT Elektronik A/S, where he worked with optical fiber measuring equipment and coherent communication systems. Since 1995, he has been with DSC Communications A/S, recently renamed to Tellabs Denmark A/S, working with SCMA-PON systems and currently with optical WDM systems.